AIAA JOURNAL
Vol. 34, No. 3, March 1996

Step Response of Pressure-Sensitive Paints

Bruce F. Carroll,* John D. Abbitt,† and Erik W. Lukas‡
University of Florida, Gainesville, Florida 32611-6250
and
Martin J. Morris§
McDonnell Douglas Aerospace, St. Louis, Missouri 63166

An experimental and analytical characterization of the response of three typical pressure-sensitive paint (PSP) formulations to a step change in pressure is presented. The three PSP formulations tested have all been previously used in wind-tunnel experiments and have been shown to have acceptable aerodynamic surface properties and mechanical durability. The time response of the PSP coatings is dependent on the diffusion of oxygen through the PSP binder material with typical time constants ranging from 0.05 to 2.5 s. The PSP response is best characterized by a two-term exponential decay function representing a complex first-order dynamic system. In contrast, a standard pressure transducer responds as a second-order dynamic system. The two-exponential curvefit provides a convenient way to compare the time response of different PSP formulations. A mass diffusion model of the PSP response is also presented that is capable of predicting the time response of PSP layers.

Nomenclature

A_i	= constant in mass diffusion solution, Eq. (7)
a	= binder layer thickness
B	= constant in two-exponential curvefit, Eq. (10)
C_1, C_2	= constants in two-exponential curvefit, Eq. (10)
D_m	= mass diffusivity, Eq. (5)
f_1, f_2	= functional relationships
I	= light intensity
N, n	= mass concentration in the binder layer
P	= pressure
R	= calibration constant, Eq. (1)
S	= calibration constant, Eq. (1)
x	= distant above the substrate
$\varepsilon_1, \varepsilon_2$	= exponential decay terms, Eq. (10)
λ	= wavelength
λ_i	= eigenvalues in mass diffusion solution, Eq. (7)
σ	= Henry's constant, Eq. (2)
τ_1, τ_2	= time constants, Eq. (10)
τ	= time constant, Eq. (8)

Subscripts

atm	= atmospheric condition
e	= excitation light source
eff	= effective value for nonequilibrium mass concentration distributions
min	= initial condition before step increase
max	= final condition after step increase
O_2	= oxygen
ref	= reference condition

Introduction

THE pressure-sensitive paint (PSP) technique is a new experimental method for the quantitative measurement of pressure on aerodynamic surfaces. PSPs are luminescent surface coatings or paints for which the luminescence intensity is inversely related to the oxygen concentration within the layer. The coatings consist of oxygen sensitive luminescent probe molecules dispersed in an oxygen permeable polymer binder.

This technology originated with the qualitative surface visualization technique presented by Peterson and Fitzgerald.[1] Advances in image processing equipment along with improvements in the chemical compositions of the luminescent coatings have led to quantitative PSP measurements with accuracies comparable to conventional pressure transducers.[2–4] Major advantages of the technique are high spatial resolutions, global measurement of a continuous surface pressure field, simplified model construction, along with the potential for high-frequency response.[2,5] McLachlan et al.[5] observed that the time response may be as fast as the luminescence decay time, on the order of 0.1 ms for platinum octaethyporphryin (PtOEP) probe molecules, but is limited by the oxygen diffusion through the polymer binder layers currently employed.

Previous research on PSP technology was focused mainly on steady-state measurements and the attendant difficulties with paint durability, surface roughness, illumination, image capture techniques, calibration procedures, temperature compensations, and image registration.[2–8] Baron et al.[9] investigated the time response of several PSP coatings but focused mainly on formulations that have not been proven for use in wind-tunnel testing. In actual wind-tunnel testing, the PSP coatings must have surface properties that do not alter the aerodynamic characteristics of the substrate. They must also have sufficient durability to remain attached to the substrate throughout the test. This paper is a characterization of the time response of three PSP formulations that have been successfully used for wind-tunnel testing and is an important step toward the routine application of PSP in unsteady pressure fields. A convenient means for equitably comparing the time response of different PSP formulations is also presented.

PSP Theory

Detailed discussions of the theory behind PSP measurements have been previously presented[2–4] and are only briefly described here. The existing theoretical framework is suitable for steady-state measurements in which the oxygen concentration through the paint layer is in static equilibrium. The unsteady characteristics of PSP are largely determined by the diffusion of oxygen through the binder layer. Accordingly, a description of the unsteady diffusion process is included.

The PSP consists of a dispersion of luminescent probe molecules in an oxygen permeable binder layer as shown in Fig. 1. An excitation light source of wavelength λ_e and intensity I_e is used to

Presented as Paper 95-0483 at the AIAA 33rd Aerospace Sciences Meeting, Reno, NV, Jan. 11–14, 1995; received Feb. 15, 1995; revision received July 21, 1995; accepted for publication Aug. 1, 1995.

*Associate Professor, Department of Aerospace Engineering, Mechanics and Engineering Science, 231 Aerospace Building. Member AIAA.
†Assistant Professor, Department of Aerospace Engineering, Mechanics and Engineering Science, 231 Aerospace Building. Member AIAA.
‡Graduate Assistant, Department of Aerospace Engineering, Mechanics and Engineering Science, 231 Aerospace Building.
§Principle Technical Specialist, Mail Code 106-7126, P.O. Box 516. Member AIAA.

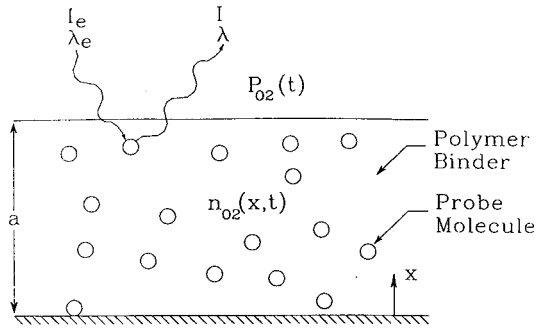

Fig. 1 Typical PSP coating (type 1 or 3) showing the coordinate system for the mass diffusion analysis.

promote the probe molecules to an excited energy state. For PSP there are two desirable mechanisms for the molecule to return to the ground state: luminescence, at wavelength λ, and intensity I, or the transfer of energy by collision with an oxygen molecule, a process called dynamic or oxygen quenching. An increase in pressure P causes a corresponding increase in the partial pressure of oxygen P_{O_2} and an increase in the oxygen concentration within the binder layer n_{O_2}. This results in a larger level of oxygen quenching and lower luminescence intensity. The luminescence wavelength is red shifted relative to the illumination wavelength allowing optical separation of the two signals. Assuming an isothermal PSP layer, the data reduction equation may be written as[2]

$$P = R(I_{\text{ref}}/I) + S \tag{1}$$

where P is the pressure above the paint layer, I_{ref} is the measured luminescence intensity at a constant reference pressure, I is the measured luminescence intensity at pressure P, and R and S are calibration constants. Depending on the exact PSP formulation, R and S display varying degrees of temperature dependence. Equation (1) is derived from the Stern–Volmer relation assuming that the polymer layer obeys a linear form of Henry's law.[2,4] Henry's law states that the concentration of oxygen in a liquid layer, n_{O_2}, is linearly proportional to the partial pressure of oxygen above the liquid, P_{O_2}, and is written as

$$n_{O_2} = \sigma P_{O_2} \tag{2}$$

Henry's constant σ also displays a temperature dependence. For a polymer layer Henry's law takes on a quadratic dependence on P_{O_2}; however, the quadratic dependence is weak, and we will follow the standard practice of assuming Eq. (2) adequately describes the layer.

A static calibration procedure is normally followed in which both P and I are measured at a series of pressures over the pressure range of interest. The term I_{ref} is generally taken as the intensity measured at $P = P_{\text{atm}}$ or some other convenient reference condition. Sufficient settling time is allowed at each pressure level to ensure a uniform oxygen concentration across the layer. A least-squares curvefit is then used to obtain the calibration constants R and S. Any nonlinearities in the response of either the paint or the photodetector are accounted for by using a higher order analogy to Eq. (1), which we will present as a general functional relation,

$$P = f_1(I_{\text{ref}}/I) \tag{3}$$

since the exact form is facility dependent. Equation (3) includes the facility-dependent effects. A second useful functional relationship is that between I/I_{ref} and P, without inclusion of the facility dependent influences, which is represented by

$$I/I_{\text{ref}} = f_2(P) \tag{4}$$

Equation (4) is obtained by a static laboratory calibration of the PSP layer using a linear photodetector and a stable illumination source. Illumination intensity must also be maintained at low levels to avoid photodegradation effects. Both Eqs. (3) and (4) assume that the oxygen concentration across the layer is the static equilibrium value for the air pressure, i.e., n_{O_2} is constant across the layer and depends only on P. This leads to an error in measuring unsteady pressure fields since, under these conditions, the oxygen concentration is not in static equilibrium.

For an unsteady pressure field, the pressure above the layer is a function of time, $P(t)$, causing the oxygen concentration inside the layer to depend on both time and distance from the plate, $n_{O_2}(x, t)$. The unsteady oxygen concentration distribution may be found by solving the mass diffusion equation,

$$\frac{\partial^2 n_{O_2}}{\partial x^2} = \frac{1}{D_m}\frac{\partial n_{O_2}}{\partial t} \tag{5}$$

where D_m is the mass diffusivity. Any binder layer that exhibits an inductive effect[10] will complicate the analysis during the initial illumination period requiring a correction term in Eq. (5). The inductive effect is characterized by a continuously increasing luminescence intensity during the initial illumination period. Uibel et al.[10] explain this effect by the interaction of the binder material with the highly reactive singlet oxygen excited by the quenching process, which makes the oxygen unavailable for further quenching of the probe molecule.

To solve Eq. (5), consider a step change in the air pressure with initial pressure $P(0) = P_{\min}$ and final pressure $P(t) = P_{\max} = \text{const}$ for all $t > 0$. The boundary conditions are derived from the assumptions of a well-mixed gas at $x = a$, i.e., no concentration gradients in the air and an impermeable wall at $x = 0$. The initial condition comes from assuming that the layer is initially in equilibrium with the air. The resulting boundary and initial conditions are

$$\begin{aligned} n_{O_2}(a, t) &= N_{\max} \\ \frac{\partial n_{O_2}}{\partial x}(0, t) &= 0 \\ n_{O_2}(x, 0) &= N_{\min} \end{aligned} \tag{6}$$

where $N_{\min} = 0.21\sigma P_{\min}$ and $N_{\max} = 0.21\sigma P_{\max}$ (0.21 is the mole fraction of oxygen in air). These boundary conditions may be transformed to homogenous boundary conditions through a transformation of variables to $\theta = (N_{\max} - n_{O_2})$. The solution to Eq. (5) subject to the boundary and initial conditions, Eq. (6), is obtained using the method of separation of variables, yielding

$$\frac{n_{O_2}(x, t) - N_{\min}}{N_{\max} - N_{\min}} = 1 - \sum_{i=1}^{\infty} \left\{ A_i \cos(\lambda_i x) \exp\left(-\lambda_i^2 D_m t\right) \right\} \tag{7}$$

where

$$\lambda_i = \left(\frac{2i-1}{2a}\right)\pi \qquad A_i = \frac{-2(-1)^i}{a\lambda_i}$$

This function describes the variation of the oxygen concentration through the binder layer. The luminescence output of the probe molecules also varies across the layer in direct proportion to the local oxygen concentration. Summing the luminescence response through the layer gives the computed response for the entire layer at a point.

Based on this model, Eq. (7) is used to make an analytical prediction of the PSP response to an unsteady pressure field. To allow for a comparison with experimental data, the concentration $n_{O_2}(x, t)$ is converted to an effective pressure, $P_{\text{eff}}(x, t)$, in the layer by applying Henry's law, Eq. (2). Using the laboratory calibration represented by Eq. (4), with local pressure $P = P_{\text{eff}}(x, t)$, we then calculate the luminescence intensity distribution across the layer, $I/I_{\text{ref}}(x, t)$. This intensity distribution is then integrated across the layer to give a prediction of the total intensity ratio. Recalling that Eq. (4) was obtained by measuring the luminescence intensity for static equilibrium oxygen concentration distributions, we see that substituting the predicted total intensity ratio allows us to compute the predicted air pressure for comparison with the PSP experimental results.

Experimental Setup

A small test cell has been constructed in which a series of experiments have been performed to determine the response of a typical PSP coating to a step change in pressure at isothermal conditions. The painted surface has dimensions of 76.2 × 6.35 mm and is separated from the transparent cover plate by a 3.18-mm-thick spacer plate. A tungsten-halogen lamp is used to illuminate the test cell and a photomultiplier tube (PMT) is used as the photodetector. The entire assembly is shown schematically in Fig. 2. The tungsten-halogen lamp is located in a fan-cooled housing to maintain a constant operating temperature. Short-term variation in the output intensity (light ripple) is rated at 0.04% rms. The long-term stability of the lamp power supply is 0.2% over 8 h after the initial 30-min warm-up period. The PMT is an integral photomultiplier tube, power supply, and amplifier with a spectral range of 185–900 nm. Four ports are located on the back side of the test cell. One is attached to a vacuum system to draw the test cell down to approximately 0.7 kPa. A second port may be opened to atmosphere through a manual toggle valve. The two remaining ports are attached to a secondary pressure standard and to a high-frequency response conventional pressure transducer. An electronic manometer with an uncertainty of ±0.28 kPa was used for the secondary standard and was connected through a valve so that it could be isolated from the system, minimizing the volume, for the step response tests. The conventional pressure transducer used during the test was a miniature silicon diaphragm strain gauge design with resonant frequency of 500 kHz (useful frequency range of 100 kHz). The PSP coating thicknesses were measured with an eddy current based nondestructive gauge. The amplified voltage output of the PMT and the conventional pressure transducer were sampled at 20 kHz per channel with a 12-bit A/D board.

Calibrations of both the PSP coating and the conventional transducer were performed in a quasistatic manner as described earlier. A linear least-squares curvefit worked well with the conventional transducer giving a standard error of estimate of ±0.28 kPa (95% confidence level, includes uncertainty from curvefit and the secondary pressure standard). The PMT/amplifier voltage output was found to be a nonlinear function of input intensity. Measurements using a cooled charge-coupled device (CCD) camera typically require a second-order polynomial calibration. Since the CCD camera has a very linear response, this indicates that the PSP responds as a second-order function of pressure. Given these two nonlinear effects, we found that a fourth-order calibration curve for Eq. (3) gave good results with an average standard error of estimate of ±0.83 kPa (95% confidence level, includes uncertainty from curvefit and the secondary pressure standard). The reference intensity was taken as an average between measurements at $P = P_{atm}$ immediately before and after the calibration. The same reference intensity procedure was used for the actual runs that were performed just following the calibration. These procedures were found to substantially reduce bias errors due to long-term drift in the voltage output of the measurement system caused by changes in illumination intensity, drift in the PMT circuitry, drift in the conventional transducer output, and photodegradation of the PSP lumiphores. Thus, an estimate of the bias error over the entire range of interest is given by the calibration curvefit's standard error of estimate given earlier.

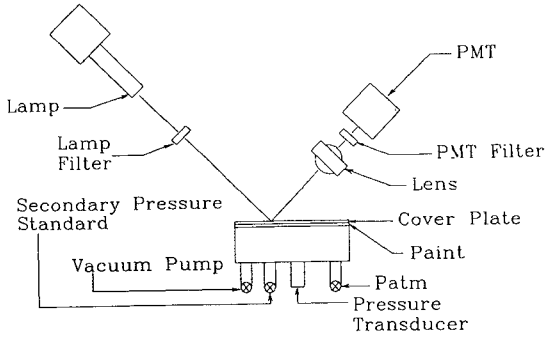

Fig. 2 Experimental setup; lamp bandpass filter centered at 450 nm and PMT bandpass filter centered at 650 nm.

Results

Three PSP formulations were used for the experiments: type 1, type 2, and type 3. Type 1 coatings consist of a proprietary probe molecule uniformly dispersed through a polymer binder layer and coated on top of a white primer layer.[2,6] Type 2 consists of PtOEP probe molecules sprayed over the top of a white primer layer. This concentrates the probe molecules near the outer surface of the type 2 PSP and is intended to improve the time response of the coating. The type 3 coating was prepared following the procedures of Kavandi et al.[3] It contains PtOEP uniformly dispersed in Genesse Polymers GP-197 dimethylsiloxane polymer and applied to a white epoxy-based primer (Krylon® spray paint). Because of the method of producing the type 2 coating (lumiphores concentrated at the outer surface), its time response should not depend on coating thickness. However, the time response of both the types 1 and 3 coatings (lumiphores uniformly dispersed through the binder layer) should have a strong dependence on thickness. The type 3 coating also exhibits an inductive effect that alters the luminescence intensity during the initial light exposure period.[10] The inductive effect is not observed in the type 1 or 2 coatings and has been accounted for in the type 3 measurements. A series of experiments were performed comparing the types 1, 2, and 3 formulations to the conventional transducer. Four type 1 thicknesses (35, 25, 15, and 13 μm), one type 2 thickness (19 μm), and three type 3 thicknesses (32, 26, and 22 μm) were tested. The measured thicknesses are the combined thickness of the primer layer and binder layer with an overall uncertainty of ±3 μm. The primer layer thicknesses were approximately 10 μm thick for the type 1 samples and 15 μm thick for the type 3 samples. The type 2 coating does not have a separate primer layer.

For each of the eight test cases the test cell was evacuated to a minimum pressure P_{min} of approximately 0.7 kPa and then vented to a maximum pressure of $P_{max} = P_{atm}$. Output from the conventional transducer and the PMT were digitized at a rate of 20 kHz per channel. Every 100 points in the output data files were then time averaged to smooth the data giving an effective sampling rate of 200 Hz per channel.

The data are presented in Figs. 3–5 in a dimensionless format consistent with the analytical model, Eq. (7). The output of the conventional transducer is used as a reference with the actual pressure rise for each experiment occurring in approximately 0.024 s. In these figures the PSP output data from the PMT has been further smoothed to filter the shot noise. The shot noise is not an important factor at the lower pressures due to higher luminescence intensity but becomes important at the high pressures due to the lower luminescence intensity. The thinner paint layers have a lower intensity output due to fewer probe molecules in the layer, which compounds the effects of shot noise and causes a higher overall uncertainty in their results. Thus, a single error band is not possible for the PSP results, rather an error band at the maximum and minimum pressure levels for each thickness is presented in Table 1. The error bands include the effects of the calibration uncertainty (bias errors) and the signal noise (precision error). Errors due to temperature effects were not considered since the coatings were maintained at a constant temperature during the tests. A detailed discussion of the

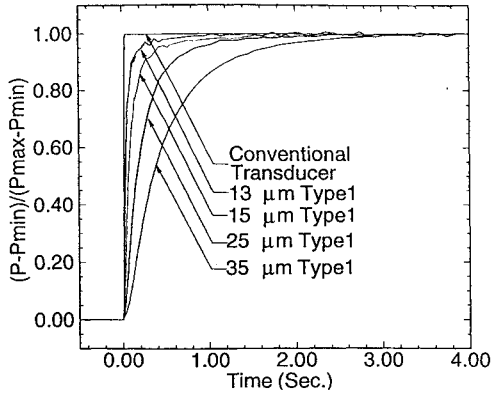

Fig. 3 Response of the type 1 coatings to a step change in pressure.

Table 1 Error bands for Figs. 3–5 with 95% confidence levels

	@P_{max}	@P_{min}
Conventional transducer	0.01	0.01
35 μm ± 3 μm type 1	0.02	0.01
25 μm ± 3 μm type 1	0.02	0.01
15 μm ± 3 μm type 1	0.04	0.01
13 μm ± 3 μm type 1	0.04	0.01
19 μm ± 3 μm type 2	0.03	0.01
32 μm ± 3 μm type 3	0.01	0.01
26 μm ± 3 μm type 3	0.01	0.01
22 μm ± 3 μm type 3	0.01	0.01

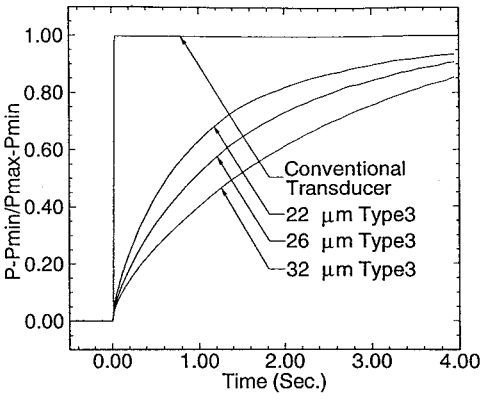

Fig. 4 Response of the type 3 coatings to a step change in pressure.

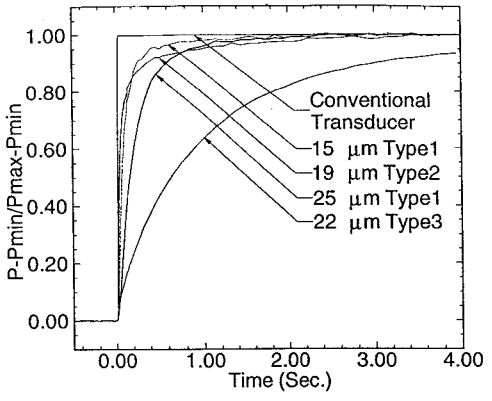

Fig. 5 Comparison of the types 1, 2, and 3 coating responses to a step increase in pressure.

uncertainty calculations is presented by Lukas.[11] Multiple experiments with each paint sample confirmed the repeatability of the experiments to within the quoted uncertainties. Caution must be used in extending these results to other PSP coatings since differences in PSP formulations and application methods can affect the resulting time response.

Turning attention to Fig. 3, we see an improvement in the rise time of the type 1 PSP as the layer thickness decreases. This results from the longer time required for oxygen to diffuse through the thicker paint layers. The 13-μm type 1 layer reaches the final pressure in approximately 1 s whereas the 35-μm type 1 layer takes approximately 3 s to reach the final pressure. Similar behavior is observed in Fig. 4 for the type 3 PSP coatings. The time response of the type 3 coatings is significantly slower than the type 1 coatings of comparable thickness. The type 3 coatings require approximately 9 s to reach the final steady-state value.

In Fig. 5, the 19-μm type 2 layer is compared with a 15-μm type 1 coating, a 25-μm type 1 coating, and the 22-μm type 3 coating. Even though the 19-μm type 2 layer is thicker than the 15-μm type 1 coating, it has a faster initial response. However, after approximately 0.2 s the 19-μm type 2 layer actually responds slower than the 15-μm type 1 coating. This observation illustrates the deficiency of using a

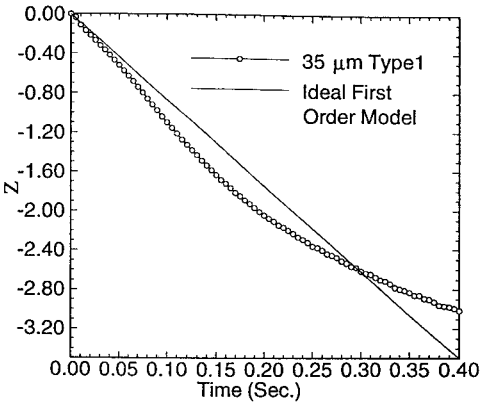

Fig. 6 Comparison of an ideal first-order dynamic system with the 35-μm type 1 coating.

90% response time as a comparison for the time response of different PSP formulations. The physical reason for the unusual behavior of the type 2 coating is unknown. We speculate that it is due to the diffusion of lumiphore molecules into the binder material so that the type 2 PSP consists of a fast responding surface layer of lumiphores and a slower responding subsurface layer of diffused lumiphores. The 25-μm type 1 is compared with the thinnest type 3 coating tested (22 μm). Recall that the type 3 primer layer is thicker than the type 1 primer layer, thus the 22-μm type 3 layer has a considerably thinner binder (or active) layer, leading one to speculate that the 22-μm type 3 coating would have faster response than the 25-μm type 1 coating. However, the type 1 layer is observed to respond quicker, with the 25-μm type 1 coating reaching steady state at about the same time as the type 2 PSP, but the 22-μm type 3 layer taking much longer. The time response of the type 3 coating is comparable to that found by Baron et al.[9] (2.5-s 90% response time) for a type 3 coating of unknown thickness. In spite of the different time responses of the various coatings, all of the coatings have a generally similar exponential type response as would be expected for a diffusion process.

The conventional pressure transducer employed is a miniature diaphragm type that responds as a second-order dynamic system, similar to a spring-mass-damper mechanical system. The PSP responds more as a first-order dynamic system as will be shown next following the procedures of Doebelin.[12] Assume a first-order response to a step change in pressure given by

$$\frac{P - P_{min}}{P_{max} - P_{min}} = (1 - e^{-t/\tau}) \tag{8}$$

where P is the pressure derived from the PSP measurements, P_{max} is the final pressure, P_{min} is the initial pressure, τ is the time constant, and t is time. This expression is similar in form to the diffusion model for the PSP layer, Eq. (7). Rearranging and taking a natural log of the equation gives

$$Z = \frac{-t}{\tau} = \ell_n\left(1 - \frac{P - P_{min}}{P_{max} - P_{min}}\right) \tag{9}$$

Plotting Z vs time for an ideal first-order system will give a straight line with the slope of the line equal to the negative inverse of the time constant. A time constant may be defined by fitting a straight line through the experimental data as has been done in Fig. 6 for the 35-μm type 1 layer. The PSP does not behave exactly as an ideal first-order system, as may be expected by comparing the ideal first-order response, Eq. (8), with the PSP diffusion model, Eq. (7). Using the linear curvefit to the data presented in Fig. 6 would give a misleading estimate of the time constant for the PSP since the slope is dependent on the time domain chosen. This is consistent with the findings of Baron et al.,[9] who found that a single-exponential model did not adequately represent the response of a type 3 formulation. The form of Eq. (7) suggests that a summation of exponential terms would provide a good representation of the PSP response.

Table 2 Two-exponential curvefit parameters

	B	C_1	τ_1, s	C_2	τ_2, s
35-μm type 1	1.0	0.99	0.42	0.11	2.4
25-μm type 1	1.0	0.99	0.20	0.084	1.2
15-μm type 1	1.0	1.0	0.084	0.074	0.88
13-μm type 1	1.0	1.1	0.042	0.058	0.48
19-μm type 2	1.0	0.95	0.045	0.16	0.82
32-μm tyoe 3	1.1	0.068	0.082	0.97	2.4
26-μm type 3	0.98	0.11	0.29	0.84	1.6
22-μm type 3	0.97	0.34	0.47	0.60	1.4

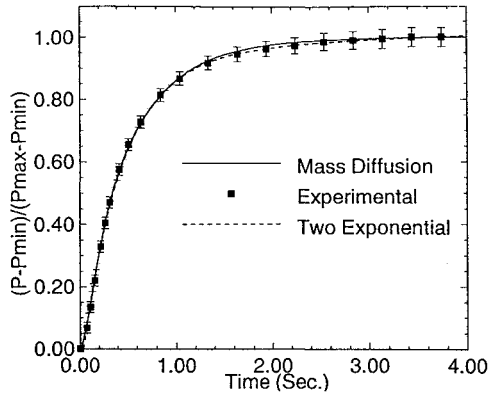

Fig. 7 Comparison of the mass diffusion model and the two-exponential curvefit to the 35-μm type 1 experimental results.

Combining two exponential terms gives the function

$$\frac{P - P_{\min}}{P_{\max} - P_{\min}} = B - [\varepsilon_1 + \varepsilon_2] \tag{10}$$

where

$$\varepsilon_1 = C_1 e^{-t/\tau_1} \qquad \varepsilon_2 = C_2 e^{-t/\tau_2}$$

This two-exponential function was found to accurately characterize all of the experimental data. Normally, the constraints $B = 1$ and $C_1 + C_2 = 1$ would be imposed. Difficulties arise from imposing these constraints in this case since the data sets have an initial concave upward curvature with an inflection point at approximately 0.05 s due to the finite rise time (0.024 s) for the pressure in the test cell. Therefore, we have not imposed these restrictions, giving a more robust curve-fitting procedure. Baron et al.[9] accounted for the finite rise time effects using a convolution integral. However, they still had difficulty fitting a two-exponential model to their type 3 coating and resorted to quoting the 90% response times. Their convolution integral method worked well for other fast coatings they tested. Since these fast coatings have not been demonstrated in wind-tunnel testing, they were not considered in this investigation. A Levenberg–Marquardt least-squares curve-fitting routine was used with Eq. (10) to obtain the constants B, C_1, C_2, τ_1, and τ_2 given in Table 2.

The two-exponential curvefit for the 35-μm type 1 layer is shown in Fig. 7 along with the results using the mass diffusion model, Eq. (7). The mass diffusion computation was performed with a mass diffusivity of $D_m = 9.0 \times 10^{-6}$ cm^2/s, which is comparable to published values for vulcanized silicone rubbers. We see that the mass diffusion model has the potential of predicting the time response of the PSP layer, assuming accurate measurements of the mass diffusivity for the binder layers are available.

A second difficulty in using the mass diffusion model is that the distribution of probe molecules through the layer must be known. This complicates application of the mass diffusion model to type 2 formulations that have a higher concentration of probe molecules near the outer surface. The two-exponential curvefit gives better agreement with the experimental data than does the mass diffusion model. However, the two-exponential curvefit is not predictive and must be obtained from measurements on an experimental sample.

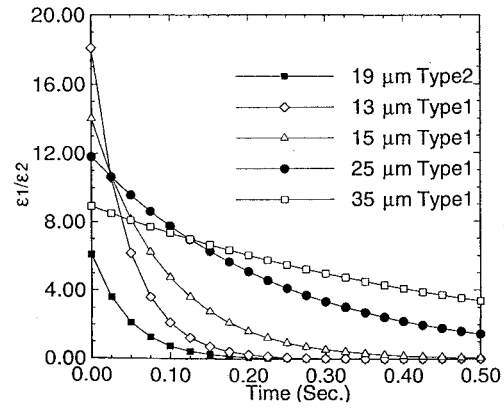

Fig. 8 Exponential decay ratio, $\varepsilon_1/\varepsilon_2$, based on the two-exponential curvefit for the types 1 and 2 formulations.

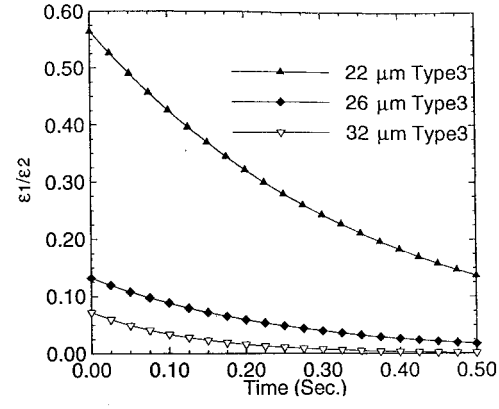

Fig. 9 Exponential decay ratio, $\varepsilon_1/\varepsilon_2$, based on the two-exponential curvefit for the type 3 formulation.

An advantage of the two-exponential curvefit is simple implmentation. It is easily applied to PSP formulations that do not have uniform probe molecule distributions through the layer (e.g., type 2 coatings) or for those with unknown mass diffusivity. The two-exponential model also provides a convenient way of comparing the time response of different PSP formulations and may be used as an index of merit for evaluating PSP time response. For our applications, constant B always has a value near unity. Looking at the other four constants we see that a fast responding PSP formulation must have small values for both time constants τ_1 and τ_2. The constants C_1 and C_2 are important in determining the relative dominance of the two time constants over different portions of the time domain.

The time constants τ_1 and τ_2 control the initial and final exponential decay rates, respectively. This is seen by looking at the ratio of the exponential decay terms, $\varepsilon_1/\varepsilon_2$, plotted in Fig. 8 (types 1 and 2) and Fig. 9 (type 3), for the first 0.5 s. Initially, at time $t = 0$, $\varepsilon_1/\varepsilon_2$ has a value greater than one for the types 1 and 2 PSP, indicating that the first exponential decay term ε_1 and corresponding time constant τ_1 have a greater influence. As time progresses, the ratio $\varepsilon_1/\varepsilon_2$ decreases until eventually ε_2 and τ_2 dominate. All of the type 1 formulations behave in a similar manner. The thinner type 1 layers have a higher initial exponential decay ratio with the transition to ε_2 dominance occurring sooner. The thinner layers also have smaller time constants τ_1 and τ_2. These characteristics are consistent with the quicker overall time response of the thinner type 1 layers displayed in Fig. 3.

The type 2 formulation behaves in a much different manner. As shown in Fig. 5, the 19-μm type 2 layer and the 15-μm type 1 layer have comparable overall response times. However, the type 2 coating has a quicker initial response, given by its smaller τ_1 for nearly equal C_1, followed by a slower final response. Although both formulations have comparable final time constants τ_2, the higher value for C_2 in the type 2 coating causes an earlier transition to τ_2 dominance. The exponential decay ratio, $\varepsilon_1/\varepsilon_2$, for the type 2 layer

shows that the initial decay term is dominant for roughly the first 0.08 s compared with 0.24 s for the 15-μm type 1 layer.

The type 3 formulation also has a surprisingly different exponential decay behavior with $\varepsilon_1/\varepsilon_2 < 1.0$ for the entire time domain, as shown in Fig. 9. This indicates that the faster responding (smaller time constant) ε_1 term is always dominated by the slow response ε_2 term, giving the lower overall type 3 response. These differences in performance are probably caused by the use of different probe molecules, different binder materials, and the distribution of probe molecules through the layer and will be the focus of future investigations.

Conclusions

An experimental investigation of the time response of three PSP coatings to a step change in pressure has been performed. All of the formulations considered have been successfully used in steady-state wind-tunnel tests. The time response of these PSP formulations are controlled by the diffusion of oxygen through the binder layer. Comparison to a high-frequency response conventional strain gauge pressure transducer shows the fundamentally different behavior of PSP measurements. The conventional device responds as a second-order dynamic system, whereas the PSP responds in a complex first-order manner. The physical mechanisms responsible for this complex PSP behavior have not been identified and need to be investigated. However, a two-exponential curvefit was found to accurately represent the time response of various PSP formulations, giving a much more descriptive characterization than the 90% response time. The experimentally obtained two-exponential model is ideally suited as an index of merit when comparing the time response of various PSP formulations. We speculate that the two-exponential model reflects multiple diffusion time scales caused by the presence of the lumiphore in the primer layer. This may also explain the unusual performance of the type 2 PSP coating since some of the lumiphore may have diffused deep into the coating while the majority of the probe molecules are very close to the coating surface. The diffused probe molecules would display a much slower time response than those near the surface.

An analytical solution to the mass diffusion equation also provides a good prediction of the PSP response to a step change in pressure, provided the mass diffusivity for the binder material is known. This model is suitable for predicting the time response of PSP coatings and can be extended to allow arbitrary pressure variations. The mass diffusion model is also well suited to parametric studies of the behavior of PSP coatings in a variety of fluctuating pressure conditions.

Acknowledgments

This work was supported by NASA Langley Research Center under Grant NAG-1-1486. The authors wish to thank William Sellers, who offered important insights and encouragement as technical monitor. We also thank Andy Winslow, who assisted with the curve-fitting routines and data analysis.

References

[1]Peterson, J. I., and Fitzgerald, V. F., "New Technique of Surface Flow Visualization Based on Oxygen Quenching of Fluorescence," *Review of Scientific Instruments*, Vol. 51, No. 5, 1980, pp. 670, 671.

[2]Morris, M. J., Donovan, J. F., Kegelman, J. T., Schwab, S. D., Levy, R. L., and Crites, R. C., "Aerodynamic Applications of Pressure Sensitive Paint," *AIAA Journal*, Vol. 31, No. 3, 1993, pp. 419–425.

[3]Kavandi, J., Callis, J., Gouterman, M., Khalil, G., Wright, D., Green, E., Burns, D., and McLachlan, B., "Luminescent Barometry in Wind Tunnels," *Review of Scientific Instruments*, Vol. 61, No. 11, 1990, pp. 3340–3347.

[4]Vollan, A., and Alati, L., "A New Optical Pressure Measurement System (OPMS)," *Proceedings of the 14th International Congress on Instrumentation in Aerospace Simulation Facilities*, IEEE Publication 91CH3028-8, 1991, pp. 10–16.

[5]McLachlan, B. G., Kavandi, J. L., Callis, J. B., Gouterman, M., Green, E., Khalil, G., and Burns, D., "Surface Pressure Field Mapping Using Luminescent Coatings," *Experiments in Fluids*, Vol. 14, No. 1, 1993, pp. 33–41.

[6]Morris, M. J., Benne, M. E., Crites, R. C., and Donovan, J. F., "Aerodynamic Measurements Based on Photoluminescence," AIAA Paper 93-0175, Jan. 1993.

[7]Donovan, J. F., Morris, M. J., Pal, A., Benne, M. E., and Crites, R. C., "Data Analysis Techniques for Pressure- and Temperature-Sensitive Paint," AIAA Paper 93-0176, Jan. 1993.

[8]Bell, J. H., and McLachlan, B. G., "Image Registration for Luminescent Paint Sensors," AIAA Paper 93-0178, Jan. 1993.

[9]Baron, A. E., Danielson, D. S., Gouterman, M., Wan, J. R., Callis, J. B., and McLachlan, B., "Submillisecond Response Times of Oxygen-Quenched Luminescent Coatings," *Review of Scientific Instruments*, Vol. 64, No. 12, 1993, pp. 3394–3402.

[10]Uibel, R., Khalil, G., Gouterman, M., Gallery, J., and Callis, J., "Video Luminescent Barometry: The Induction Period," AIAA Paper 93-0179, Jan. 1993.

[11]Lukas, E. W., "Pressure Sensitive Paint Response to a Step Rise in Pressure," M.S. Thesis, Dept. of Aerospace Engineering, Mechanics, and Engineering Science, Univ. of Florida, Gainesville, FL, 1995.

[12]Doebelin, E. O., *Measurement Systems Application and Design*, 4th ed., McGraw–Hill, New York, 1990, pp. 108–114.